

Electronic Supplementary Material (ESI) for ChemComm

**Magnetic-Field-Assisted Deposition of Self-Assembled Crystallite Layers
of Co²⁺-Containing Layered Double Hydroxides**

Daniel E.L. Vieira,^a João P.V. Cardoso,^a Alexey V. Fedorchenko,^b Elena L. Fertman,^b
Erik Čížmár,^c Alexander Feher,^c Roman Yu. Babkin,^d Yurii G. Pashkevich,^{*d}
Christopher M.A. Brett,^e Joaquim M. Vieira,^a Andrei N. Salak^{*a}

^a *Department of Materials and Ceramic Engineering, CICECO – Aveiro Institute of Materials, University of Aveiro, 3810-193 Aveiro, Portugal.*

^b *B. Verkin Institute for Low Temperature Physics and Engineering of the National Academy of Sciences of Ukraine, Kharkiv61103, Ukraine.*

^c *Institute of Physics, Faculty of Science, P.J.ŠafárikUniversity in Košice, Košice04154, Slovakia.*

^d *O. Galkin Donetsk Institute for Physics and Engineering, National Academy of Sciences of Ukraine, Kyiv03680, Ukraine*

^e *Department of Chemistry, CEMMPRE, Faculty of Sciences and Technology, University of Coimbra, 3004-535 Coimbra, Portugal.*

* E-mail address:

salak@ua.pt (Dr. Andrei N. Salak)

yu.pashkevich@gmail.com (Prof. Yurii G. Pashkevich)

1. Experimental section.

Cobalt (II) nitrate hexahydrate ($\geq 98\%$), aluminium nitrate nonahydrate ($\geq 98.5\%$), sodium hydroxide ($\geq 98\%$), sodium nitrate ($\geq 99.5\%$), sodium carbonate ($> 99.95\%$) were purchased from Sigma-Aldrich. The chemicals were used as received without further purification. All the solutions were prepared in deaerated water.

Parent $\text{Co}_2\text{Al-NO}_3$ LDH was synthesized by co-precipitation method, and $\text{Co}_2\text{Al-CO}_3$ LDH was obtained from the parent nitrate-intercalated by anion-exchange. Both procedures were performed under nitrogen atmosphere. Proportions of the reagents were chosen to achieve the molar cation ratio $n = 2$ without any excess.

To prepare $\text{Co}_2\text{Al-NO}_3$ LDH, a solution containing 0.5 M $\text{Co}(\text{NO}_3)_2 \cdot 6\text{H}_2\text{O}$ and 0.25 M $\text{Al}(\text{NO}_3)_3 \cdot 9\text{H}_2\text{O}$ was instilled drop-by-drop in a 1.5 M NaNO_3 solution under continuous stirring at room temperature. During the precipitation, the pH value of the mixture was kept to be 8 by addition of a 2 M NaOH solution. In order to accelerate the crystallization and homogenization of the crystallites, the obtained suspension was sonicated for 5 min using a VCX 1500 Sonics processor with a maximum output power of 1.5 kW at 20 kHz. The resulting mixture was centrifuged at 7500 rpm for 90 s. The obtained slurry was washed with deionized water followed by centrifugation. This procedure was repeated three times to remove any residual NaNO_3 .

The $\text{NO}_3 \rightarrow \text{CO}_3$ anion-exchange was conducted by mixing the $\text{Co}_2\text{Al-NO}_3$ LDH with a 0.1 M NaCO_3 solution at room temperature. The pH value of the mixture was adjusted to be 8. The mixture was sonicated at 1.5 kW for 7 min and then centrifuged at 7500 rpm for 90 s.

$\text{Co}_2\text{Al-NO}_3$ and $\text{Co}_2\text{Al-CO}_3$ LDH were obtained in the form of dense slurry that contained about 80% of water. For phase identification by XRD, the slurries were dried for 12 hours at 60°C .

Prior to the deposition procedure, an LDH slurry was mixed with ethanol (0.01 g per 1 ml of ethanol) and dispersed for 15 min using an ultrasonic bath. The obtained suspension was put in a flat 10 mm height plastic container with a 15×15 mm substrate slab at the bottom. Two types of substrates were used: optical glass and single-crystal silicon.

The container was placed horizontally between either vertically or horizontally oriented poles of a GMW Model 3470 electromagnet connected to an Agilent Model 6811B Power Source/Analyzer. The magnetic field generated in the pole gap was 0.5 T. The field was applied in three cycles of 1 min each. The cycles were divided into pulses of 10 s for the first minute and 20 s for the next two cycles. Then the substrate with the precipitated LDH was dried in the oven at 60°C until the complete evaporation of ethanol. For comparison, the samples were also prepared using the same conditions in a zero magnetic field.

The phase content and the crystal structure of the obtained samples either in form of powder or in form of films deposited on flat substrates were characterized using a PANalytical X'Pert Powder diffractometer (Ni-filtered $\text{Cu K}\alpha$ radiation, step 0.02° , exposition time ~ 1.5 s per step) over a 2-Theta range of $5-70^\circ$ at room temperature.

Microstructure of the powder samples was investigated by scanning transmission electron microscopy (STEM) using a Hitachi HD-2700 STEM operated at 200 kV. Cross

sections of the deposited LDH layers were studied using a Hitachi S4100 scanning electron microscope (SEM) operated at 25 kV.

Magnetic properties of the deposited LDH layers were assessed using a Quantum Design MPMS3 magnetometer between 1.8 and 300 K. Static magnetic susceptibility determined as a ratio of the measured magnetic moment and applied magnetic field ($\chi=M/H$) was studied using in both zero-field-cooled (ZFC) and field-cooled (FC) modes in a magnetic field of 100 Oe. Hysteresis loops were measured at 2 K after demagnetizing the sample at ambient temperature using an oscillation field procedure and cooling in zero magnetic field. The surface area of the films used for magnetic measurement was calculated using a calibrated scale under an optical microscope.

2. Phase content and microstructure of the powder LDH samples.

Analysis of the XRD patterns of the powders obtained from the dried slurries both before and after the nitrate-to-carbonate anion exchange revealed that the obtained compositions are single-phase LDH [14]: $\text{Co}_2\text{Al-NO}_3$ and $\text{Co}_2\text{Al-CO}_3$, respectively (Fig. S1).

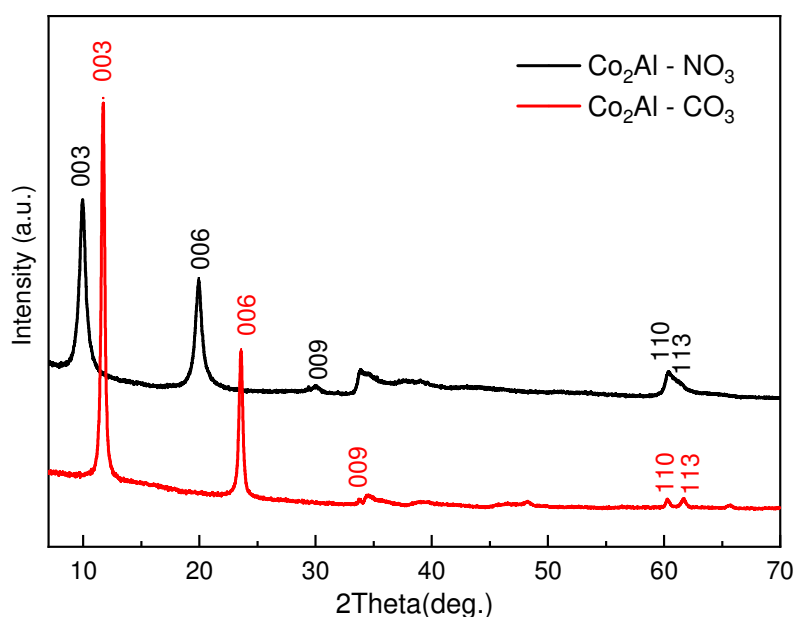


Fig. S1. XRD patterns of $\text{Co}_2\text{Al-NO}_3$ and $\text{Co}_2\text{Al-CO}_3$ LDH powders obtained from the as-prepared slurries.

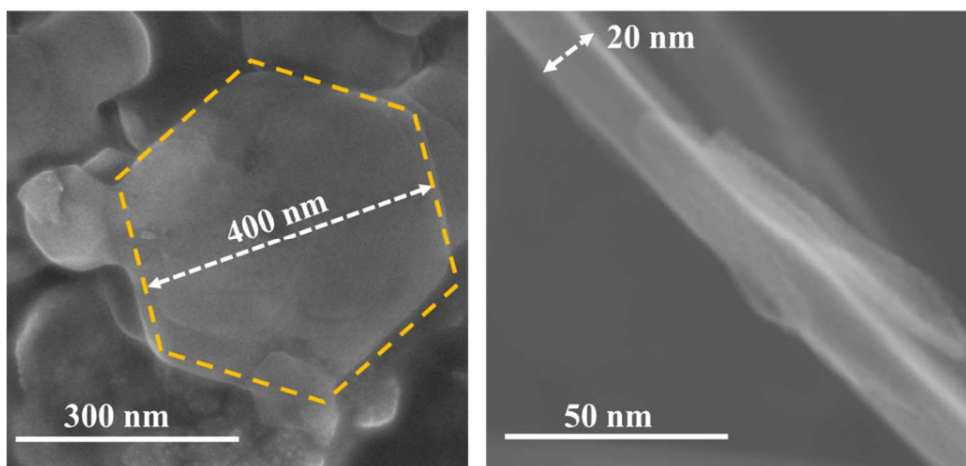


Fig. S2. STEM images of detached crystallites of $\text{Co}_2\text{Al-NO}_3$ LDH.

3. Crystal structure of the deposited layers

Considerably high intensities of the diffraction reflections of the $(00l)$ family in the XRD patterns of the $\text{Co}_2\text{Al-NO}_3$ LDH layers deposited in a magnetic field directed perpendicularly to the substrate surface indicate the preferred orientation of the LDH crystallites (parallel to the substrate surface) in these layers in comparison with rather random orientation of the crystallites in the layers deposited in a zero magnetic field (Fig. S3).

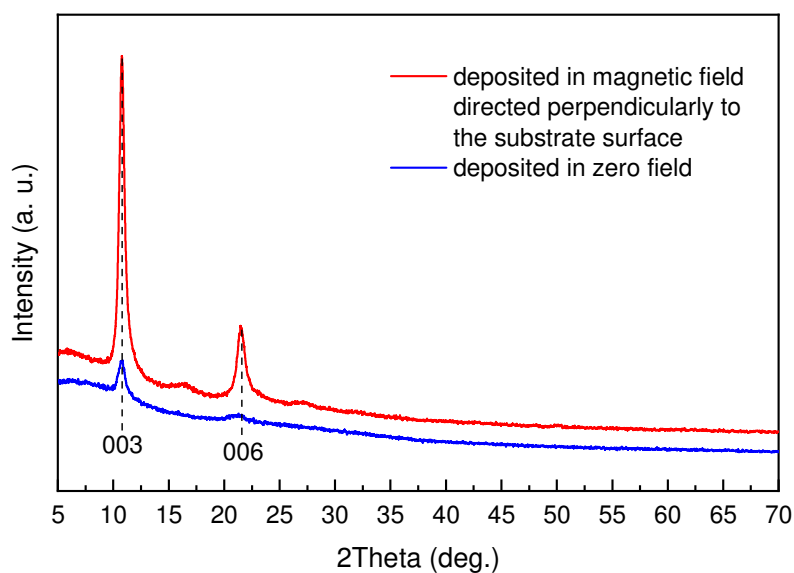


Fig. S3. XRD patterns of $\text{Co}_2\text{Al-NO}_3$ LDH layers on glass substrates deposited in a magnetic field directed perpendicularly to the substrate surface (red line) and in a zero magnetic field (blue line).

4. Magnetic behaviour of the deposited LDH layers.

In the magnetic measurements, the samples deposited on the single-crystal Si substrates were used. Due to a very weak magnetic moment of the film at the ambient temperature, the measurements were focused on the low-temperature range. First, the temperature dependence of the magnetic moment of the films was measured with a small magnetic field B_{meas} applied parallel to the substrate (to avoid the possible effect of demagnetising field). The measurements were carried out in both the zero-field cooled (ZFC) and field cooled (FC) modes. A steep increase of the magnetic moment (Fig. S4) and an onset of the hysteresis loops (Fig. S5) with decreasing temperature below 10 K are evident of the long-range ferromagnetic ordering. The Curie temperature, T_c , was determined to be about 6.5 K for all films studied, which is in a good agreement with the values obtained earlier for the powdered LDH of the same composition [14].

The maximum value of the magnetic moment detected in the films deposited in the magnetic field directed perpendicularly to the substrate surface was found to be by a factor of 10 and 4 higher than the corresponding values for the films obtained with the magnetic field applied parallel to the substrate and without magnetic field, respectively (Fig. S4). The highest value of the coercive field was also observed in the films deposited in the magnetic field directed perpendicularly to the substrate (Fig. S5). Besides, the better homogeneity of these films is demonstrated by the most rectangular (ferromagnetic-like) hysteresis loops where a simple spin flip will occur after the field reversal. The magnetization reversal of the films prepared in a parallel magnetic field has a more pronounced S-shape that reflects different spin reorientation mechanisms due to a partial preferential orientation of magnetic moments along the substrate.

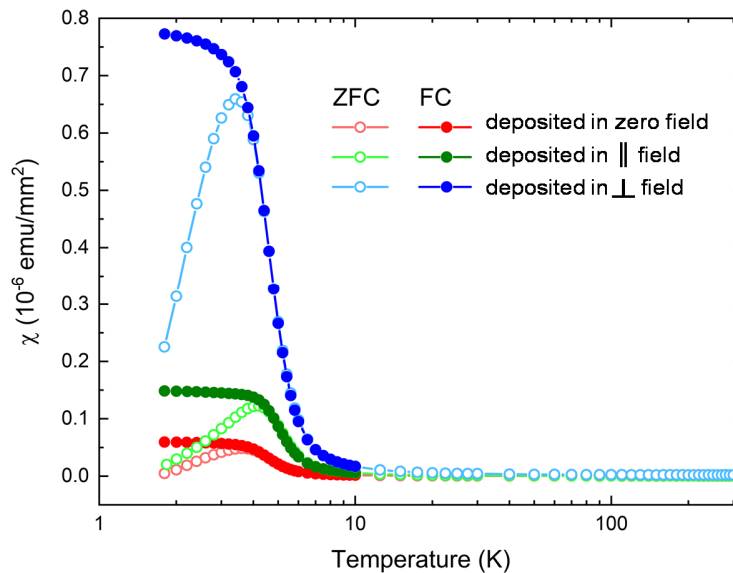


Fig. S4. Magnetic susceptibility of the $\text{Co}_2\text{Al-NO}_3$ LDH films on single-crystal Si substrates deposited in a magnetic field directed perpendicularly (blue line), parallel (green line) to the substrate surface (red line) and in a zero magnetic field (red line).

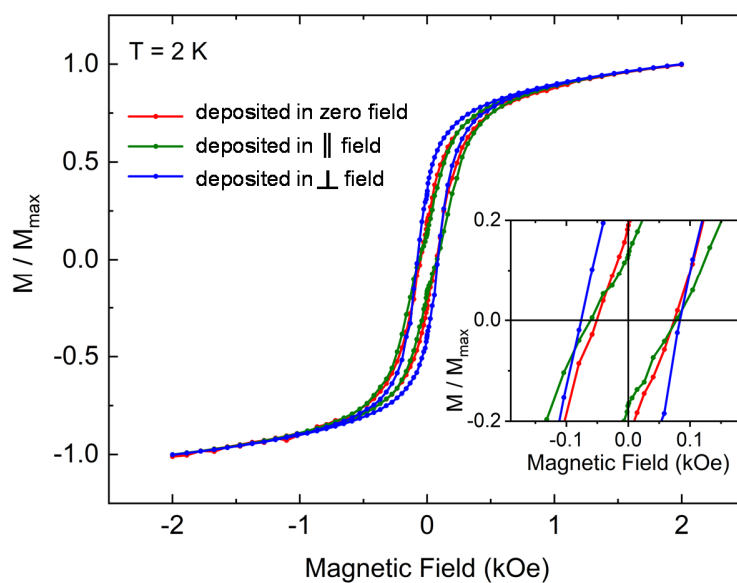


Fig. S5. Normalized magnetic hysteresis loops of the $\text{Co}_2\text{Al-NO}_3$ LDH films on single-crystal Si substrates deposited in a magnetic field directed perpendicularly (blue line), parallel (green line) or the substrate surface (red line) and in a zero magnetic field (red line). Inset shows the enlarged central part of the hysteresis loops.

5. Morphology of the deposited layers of $\text{Co}_2\text{Al-CO}_3$ crystallites.

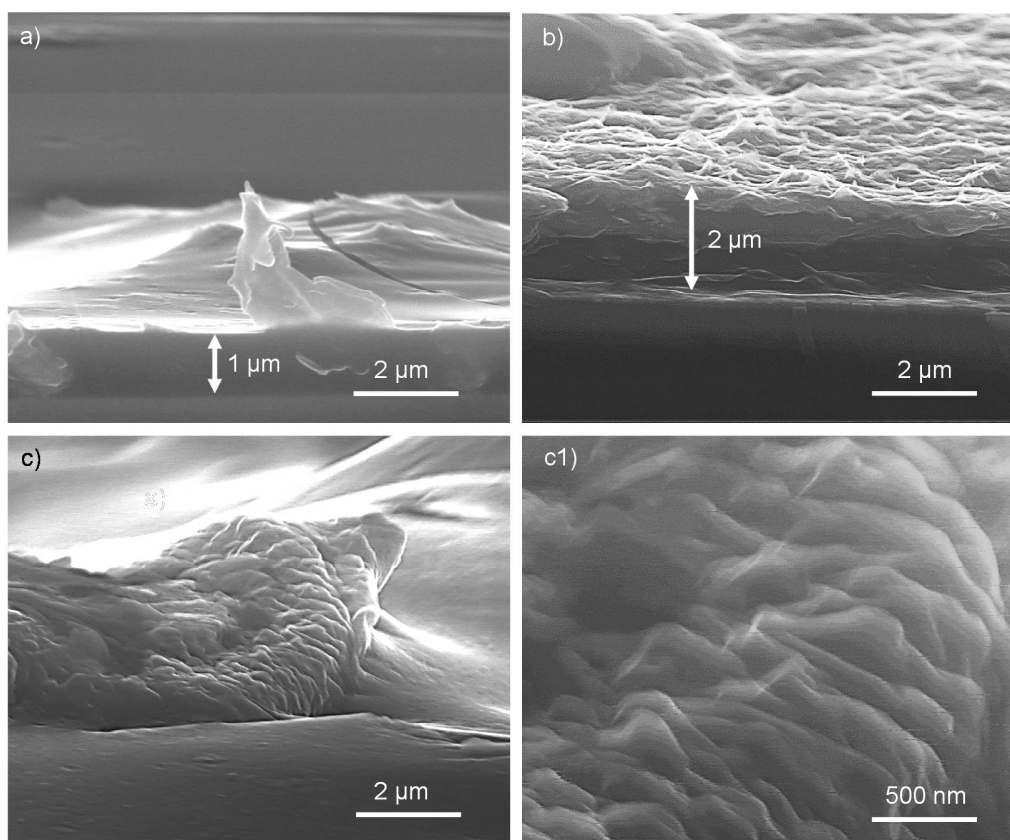


Fig. S6. SEM images (cross-section view) of layers of the $\text{Co}_2\text{Al-CO}_3$ LDH crystallites deposited on glass substrates in a magnetic field directed (a) perpendicularly to the substrate surface, (b) parallel to the substrate surface. (c) SEM image (small-angle surface view) the $\text{Co}_2\text{Al-CO}_3$ LDH layer deposited in a magnetic field directed parallel to the substrate surface with (c1) magnified area with vertical stuck crystallites.

6. Details of the theoretical calculations.

To proceed with direct calculations of the energy spectrum and g-factor values, the Modified Crystal Field Theory (MCFT), the original semi-empirical approach for calculations of the electronic structure of paramagnetic ions in coordination complexes with arbitrary symmetry and numbers of ligands [30,31] was used. The spin-orbit coupling is incorporated into MCFT and the positions of ligands, the ligands charges and the effective nuclear charge of the metal ion are the input parameters.

The energy spectra of Co^{2+} (configuration $3d^7$, basic term 4F) for all thirteen possible cobalt coordinations have been calculated using the model of distorted hydroxyls cages described in the main text, the nominal valence charges of surrounding atoms and the Co^{2+} effective nuclear charge of 6.55|e|. The high spin state of cobalt has been detected for all possible coordinations.

Table S1. Statistical weights of the possible cation coordinations (the types *a-m*) of cobalt in Co₂Al LDH [15].

Type	<i>a</i>	<i>b</i>	<i>c</i>	<i>d</i>	<i>e</i>	<i>f</i>	<i>g</i>
Weight	0.072	0.25	0.14	0.14	0.07	0.075	0.15
Type	<i>h</i>	<i>i</i>	<i>j</i>	<i>k</i>	<i>l</i>	<i>m</i>	
Weight	0.025	0.04	0.04	0.02	0.02	0.002	

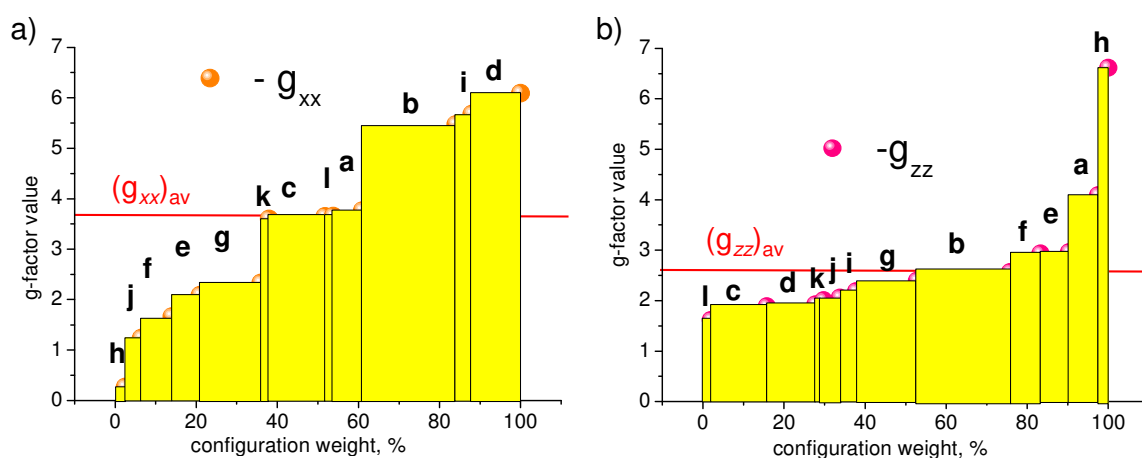


Fig. S7. Distribution of the *xx*- and *zz*- components for *g* factor of the lowest Kramers doublet among all possible cation coordinations of cobalt in Co₂Al LDH. The type of coordination denotes by the letter above rectangles. The statistical weight of each configuration is presented by rectangle's width. The red lines mark statistical average of respective *g*-factor components.

The calculated magnetic susceptibility at room temperature for each individual coordination also preserves highly anisotropic behaviour (Table S2). The respective values have been obtained by accounting for only four lowest Kramers doublets all of which are situated in the range of 0-300 cm⁻¹.

Table S2. The xx - and zz -components of magnetic susceptibility calculated at $T = 300$ K for different Co-Al coordinations.

Type	Susceptibility (emu/mol)	
	χ_{xx}	χ_{zz}
<i>a</i>	0.2043	0.2584
<i>b</i>	0.5142	0.3604
<i>c</i>	0.2872	0.3241
<i>d</i>	0.5543	0.3308
<i>e</i>	0.1058	0.4138
<i>f</i>	0.3078	0.3239
<i>g</i>	0.1430	0.3748
<i>h</i>	0.0938	0.5041
<i>i</i>	0.5446	0.3419
<i>j</i>	0.1115	0.3369
<i>k</i>	0.2708	0.3513
<i>l</i>	0.2971	0.3015